Appl. Phys. B 75, 367–376 (2002)
DOI: 10.1007/s00340-002-0991-8

Applied Physics B
Lasers and Optics

M.W. TODD[1,✉]
R.A. PROVENCAL[1]
T.G. OWANO[1]
B.A. PALDUS[1]
A. KACHANOV[1]
K.L. VODOPYANOV[1]
M. HUNTER[2]
S.L. COY[2]
J.I. STEINFELD[2]
J.T. ARNOLD[3]

Application of mid-infrared cavity-ringdown spectroscopy to trace explosives vapor detection using a broadly tunable (6–8 μm) optical parametric oscillator

[1] Picarro, Inc., 1050 E. Duane Ave., Suite H, Sunnyvale, CA 94085, USA
[2] Department of Chemistry and G.R. Harrison Spectroscopy Laboratory, Massachusetts Institute of Technology, Cambridge, MA 02139, USA
[3] Varian Medical Systems, Ginzton Technology Center, Mountain View, CA 94039, USA

Received: 1 April 2002/Revised version: 13 June 2002
Published online: 12 September 2002 • **© Springer-Verlag 2002**

ABSTRACT A novel instrument, based on cavity-ringdown spectroscopy (CRDS), has been developed for trace gas detection. The new instrument utilizes a widely tunable optical parametric oscillator (OPO), which incorporates a zinc–germanium–phosphide (ZGP) crystal that is pumped at 2.8 μm by a 25-Hz Er,Cr:YSGG laser. The resultant mid-IR beam profile is nearly Gaussian, with energies exceeding 200 μJ/pulse between 6 and 8 μm, corresponding to a quantum conversion efficiency of approximately 35%. Vapor-phase mid-infrared spectra of common explosives (TNT, TATP, RDX, PETN and Tetryl) were acquired using the CRDS technique. Parts-per-billion concentration levels were readily detected with no sample preconcentration. A collection/flash-heating sequence was implemented in order to enhance detection limits for ambient air sampling. Detection limits as low as 75 ppt for TNT are expected, with similar concentration levels for the other explosives.

PACS 42.65.Yj; 42.62.Fi; 33.20.Ea; 07.07.Df

1 Introduction

On December 21st 1988, Pan Am flight 103 crashed over Lockerbie, Scotland, killing all 259 people on board and 11 on the ground. The crash resulted from the explosion of a terrorist's bomb concealed within luggage that had been checked onto the flight at Frankfurt airport. This tragedy prompted the US Federal Aviation Administration (FAA) and Congress to intensify efforts at improving security measures at airports and on passenger airline flights. During the 1990s, no other incidents of airline bombings are known to have occurred, although attacks on stationary targets (World Trade Center towers, Murrah Federal Building in Oklahoma City, U.S. embassy buildings in Nairobi and Dar es Salaam, among others) using powerful, large-volume truck bombs occurred with disturbing frequency.

Our perception of the threat changed dramatically on September 11th 2001, when coordinated attacks on four domestic U.S. flights, resulting in complete destruction of the World Trade Center buildings in New York City and extensive damage to the Pentagon, clearly demonstrated the existence of a wide-ranging conspiracy to inflict lethal damage on the citizens and property of developed countries, particularly those allied with the U.S. Several months later, an attempt to bring down a trans-Atlantic flight by detonation of explosive materials concealed in the shoes of one of the passengers on board was thwarted by the increased vigilance of the crew and other passengers on that flight. This incident further demonstrated that such attacks can take many different (and unexpected) forms, and that escape or survival of the perpetrator is not an essential requirement in planning these attacks.

While these threats exist, it will be necessary to take precautions against the introduction of substances such as explosives or chemical and biological warfare agents into vulnerable targets, especially airplanes in flight. It is not only passengers and carry-on baggage that must be screened for these substances; the Aviation and Transportation Security Act of 2001 requires *all* checked baggage to be screened by explosives detection systems (EDSs) by the end of 2002. This represents a formidable challenge to the airlines, to the Transportation Security Administration (TSA) and other security agencies, to equipment manufacturers and not least to the traveling public. At the present time, there are relatively few certified EDS techniques available for this purpose [1]. X-ray tomographic techniques have been proven effective in detecting bulk quantities of certain explosives, and are widely deployed in airport security applications [2–6]. Trace explosives detection techniques have also been developed to complement bulk detection methods, and to overcome their safety limitations when applied to the screening of human subjects. Of these, by far the most sensitive and reliable is the use of trained dogs, but this method is limited by the effective attention span of the animals, which cannot be worked continuously for more than a few hours [7, 8]. Commercial instruments based on ion mobility spectrometry (IMS) are currently in use at passenger security checkpoints for the detection of explosives [9]. The sensitivity of IMS can equal that of mass spectrometry, with detection limits as low as 30 pg of RDX and 1 ng of TNT, however the enhanced sensitivity comes at a cost of reduced selectivity. In order to minimize the false alarm rate, IMS instruments must compromise selectivity and sensitivity.

✉ Fax: +1-408/524-0551, E-mail: mtodd@picarro.com

Optical spectroscopy provides an attractive alternative for trace vapor detection of explosives for several reasons. The fact that molecules absorb light at distinct, characteristic wavelengths allows for the unique spectral identification of a chemical by measuring its absorption spectrum. Compounds in a mixture can be differentiated on the basis of their spectroscopic signatures, if necessary with the aid of pattern recognition algorithms [10]. Traditional linear absorption techniques, however, do not possess the required sensitivity for detecting compounds that have low equilibrium vapor pressures, corresponding to atmospheric mixing ratios of one part-per-billion (ppb) or less. The concealment of explosives drops the ambient concentrations well below their saturated vapor pressures, posing an even greater demand on detection sensitivity. In the case of low-vapor-pressure explosives such as trinitrotoluene (TNT), cyclotrimethylene nitramine (RDX), or pentaerythritol tetranitrate (PETN), their vapor would be difficult if not impossible to detect under normal conditions using linear absorption spectroscopic methods.

Our groups at M.I.T. and BlueLeaf Networks, Inc. are utilizing the technique of mid-IR cavity-ringdown spectroscopy (CRDS), which will improve the selectivity of explosives detection over the IMS method while matching its sensitivity and detection limits. In this paper, a background on the CRDS technique is provided in Sect. 2. Section 3 then describes the experimental set-up, including a description of a novel mid-IR optical parametric oscillator (OPO) system that provides output radiation in the required wavelength range. Results on model compounds such as TNT, RDX and PETN are presented in Sect. 4. Finally, conclusions and plans for future applications of this technique are provided in Sect. 5.

2 Background on CRDS

Cavity-ringdown spectroscopy is a highly sensitive technique for absolute measurement of species that either are weakly absorbing or have very low concentration. CRDS was first introduced using pulsed tunable lasers in the late 1980s [11] and has since been applied to a number of spectroscopic studies of extremely weak molecular transitions and for trace gas detection, both with pulsed [12–19] laser sources operating from UV to mid-IR, and with CW laser diodes [20–22]. A general description of the method, as well as additional references, can be found in a recent publication by Busch et al. [23].

The principle of CRDS is as follows. Light from a pulsed or CW laser source is injected into a stable optical cavity formed by two, or more, highly reflective mirrors. At the end of the laser pulse (or in the case of a CW laser, the laser is turned off) the intracavity radiation will decay exponentially with a time constant, τ, that is determined by the reflectivity of the mirrors, R, the scattering inside the cavity (such as Rayleigh scattering of the gas sample), and the wavelength-dependent absorption of the intracavity gas $\alpha(\lambda)$. It is expressed as,

$$\frac{1}{c\tau} = \alpha(\lambda) + \frac{n(1-R)+A}{L}\,, \tag{1}$$

where c is the speed of light, L is the roundtrip cavity length, n represents the number of cavity mirrors, and A corresponds to the round-trip loss in the cavity due to scattering. The mirrors are assumed to be identical, with a reflectivity very close to 1, so that we can use an approximation $\ln(1/R) \approx (1-R)$. The decay time can be determined to a high accuracy by monitoring the light intensity exiting one of the cavity mirrors and fitting its time dependence to a single exponential function.

From (1) we immediately see one of the most attractive features of CRDS. Once the baseline losses in an empty cavity are determined (namely the reflectivity of the mirrors, R, and other intracavity losses, A), the *absolute* absorption spectrum of the intracavity medium, $\alpha(\lambda)$, expressed in cm^{-1}, is immediately extracted by tuning the laser source, and plotting the quantity $1/c\tau$ versus the wavelength.

A significant advantage to using cavity-ringdown, particularly in this experiment, which employs a pulsed optical parametric oscillator (OPO), is that the absorption measurement is independent of laser intensity fluctuations. It can be shown that the noise in the measured absorption spectrum, and thus the minimum detectable absorption, is determined by the relative measurement error, $\delta\tau/\tau$, of the decay constant τ, and by the equivalent absorption length $c\tau$. The decay rate is independent of the intensity fluctuations of the laser source [19, 20]. Ultimately, systematic effects must also be included in determining the minimum sensitivity, however there is some analogy between CRDS and ordinary absorption spectroscopy, where the minimum detectable absorption depends on the measured relative fluctuation of the laser intensity, $\delta I/I$, and on the absorption path length, L. It has recently been shown that with the use of a properly designed cavity, mode-matching optics and a sensitive detector, it is possible to achieve a relative standard deviation of the measured decay time, $\delta\tau/\tau$, of 0.3% with a pulsed laser [20]. In a typical cavity (e.g. $L = 50$ cm, $R = 0.9999$), ringdown decay times of approximately 20 μs are routinely obtained, which is equivalent to a 6 km path length. This corresponds to a minimum detectable absorption with a single pulse per data point of $5 \times 10^{-9}\,\mathrm{cm}^{-1}$. By analogy, to achieve this sensitivity with direct absorption methods using pulsed lasers would require a laser with pulse-to-pulse fluctuations, $\delta I/I$, of 0.3% and a multi-pass cell with a 6-km path length. Neither of these is available in practice.

The OPO laser that is described in the experimental section has multiple longitudinal modes in a 2-cm^{-1} linewidth, which is well matched to the broad absorption features of explosives vapor. However, when a CRD cavity is excited with such a pulsed source, special care should be taken in order to decrease the additional noise due to the excitation of higher-order transverse modes of the cavity [15–18], and the finite spectral width of the laser source [16]. Even for a spatially filtered pulsed input, different subsets of the cavity transverse modes can be excited in different pulses due to variations of the source mode and intensity distribution. As a result, beat patterns, which vary from pulse to pulse, are superimposed with the exponential decay, producing uncertainty in the calculated decay times. Additionally, if there are species in the cavity-ringdown cell with narrow absorption lines with respect to the laser bandwidth (such as water vapor, discussed in Sect. 4.5), differences in the decay times for different excited cavity modes will result in multi-exponential decays. Fitting these multi-exponential

decays with a single exponential will also produce excess noise. Special measures must be therefore be implemented to insure single-cavity-mode excitation, and data acquisition algorithms can also account for the multi-exponential decays. With such precautions, absorption coefficients as low as $5 \times 10^{-10}\,\mathrm{cm}^{-1}\,\mathrm{Hz}^{-1/2}$ have been observed with a pulsed OPO [19], demonstrating that pulsed CRDS can approach sensitivity levels of CW CRDS.

3 Experimental

A prototype instrument has been designed to measure the absorption spectra of explosive vapor at sub-ppb concentration levels using mid-infrared CRDS. As a mid-IR tunable laser source, we used a zinc–germanium–phosphide (ZGP) optical parametric oscillator (OPO). The OPO was pumped by a Q-switched erbium- and chromium-doped yttrium–scandium–gallium–garnet (Er,Cr:YSGG) laser which delivered pulses with the following parameters: $\lambda = 2.8\,\mu\mathrm{m}$, energy 2–3 mJ, pulse duration 100 ns and TEM_{00} spatial mode. The laser was pumped by a flashlamp (typical pump energy 8–9 J) and operated at a repetition rate of 25 Hz.

An AR-coated ZGP crystal (Inrad, Inc.), 20-mm-long, and 7×10 mm in cross section, was cut at $\theta_0 = 70°$ ($\varphi = 45°$) for type-II phase-matching. The OPO cavity (Fig. 1) was formed by two mirrors, M1 and M2, which were spaced 3 cm apart. The pump laser beam size ($1/e^2$ intensity radius) was approximately 0.8 mm. The front OPO mirror, M1, was transmissive ($> 80\%$) for the pump and idler waves and was highly reflective (98%) for the OPO signal wave. A gold rear mirror, M2, highly reflected ($R > 98\%$) all three waves, namely pump, signal and idler. Thus, the signal wave resonated, while pump and idler waves were recycled – they made a double pass and exited from the OPO cavity [24]. A dichroic beam splitter (BS) separated the incoming pump beam from the outgoing idler.

Tuning of the OPO was achieved by rotating the ZGP crystal with a rotation stage (Newport SL50). The angle of the crystal was controlled by computer, through GPIB commands to the rotation stage. Figure 2 shows the OPO angular tuning curve (only the idler wave is shown), together with the predicted tuning curve from known dispersion relations [24] (solid line). Continuous tunability of 6–10 μm (idler wave) and 3.9–5.8 μm (signal wave) was achieved with a single orientation ZGP crystal and a single set of OPO mirrors.

In this work, the OPO was optimized for maximum output in the range 6 to 8 μm. Energies at 6–8 μm reached 200–300 μJ per pulse, which corresponds to a quantum conversion efficiency of approximately 35%. The OPO linewidth was typically $2\,\mathrm{cm}^{-1}$ (it was slightly smaller at shorter idler wavelengths, e.g. $1.5\,\mathrm{cm}^{-1}$ at $\lambda_{\mathrm{idler}} = 6.3\,\mu\mathrm{m}$, and slightly larger at longer wavelengths, $2.6\,\mathrm{cm}^{-1}$ at 7.7 μm).

The OPO output displayed excellent spatial beam characteristics, which were measured using a 2D infrared beam profiler (Spiricon Pyrocam I). Figure 3 shows the far-zone beam intensity distribution (at $\lambda = 6.6\,\mu\mathrm{m}$), which was close to a circular Gaussian shape with a full-width half-maximum (FWHM) of 5 mrad, corresponding to about 1.5× the diffraction limit (beam quality parameter $M^2 = 1.5$). The pointing stability was stable to 10% of FWHM. No pinhole was employed for spatial filtering due to the slight pointing instability, which greatly exacerbated pulse-to-pulse energy fluctuations after a pinhole. Nevertheless, the current beam quality was sufficient for good mode matching to the ringdown

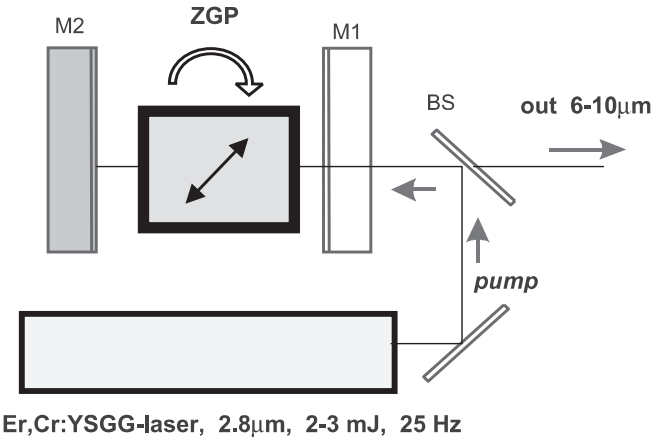

FIGURE 1 Er,Cr:YSGG-pumped ZGP OPO configuration

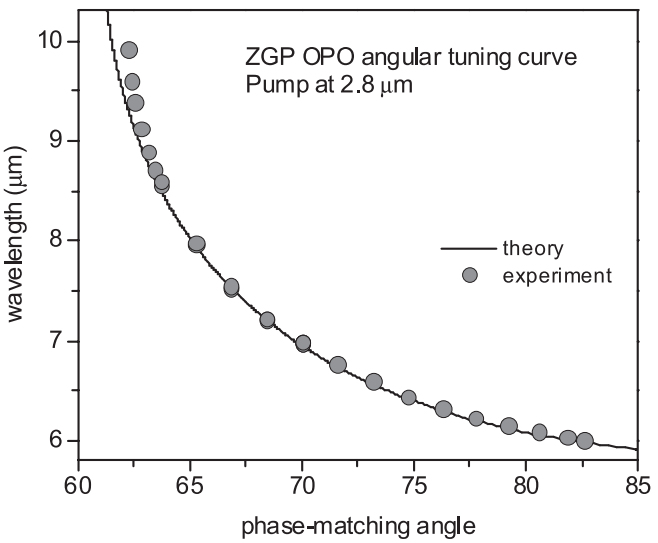

FIGURE 2 OPO angular tuning curve for the idler wave, together with the predicted curve (*solid line*)

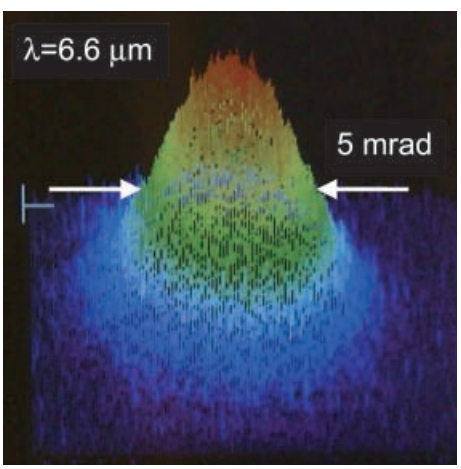

FIGURE 3 Far-zone OPO beam distribution at $\lambda = 6.6\,\mu\mathrm{m}$, taken with a Spiricon beam profiler

cavity, where a relative measurement error, $\delta\tau/\tau$, of 1% was achieved.

Figure 4 displays the experimental set-up. The CRD cell for this instrument was a simple, 50 cm linear cavity formed by two ZnSe mirrors, coated for the 7–8 μm region ($R = 0.99996$, and 0.5 m radius of curvature). In order to minimize the required sample volume, explosives vapor was injected into a 10-cm-long bore with 0.8-cm diameter (volume= 5 cm^3), located in the center of the ringdown cavity. The heated central bore was attached to the end mirror mounts with quartz tubes to allow for thermal isolation of the mirrors. The cell pressure was maintained at 100 Torr with a small flow of nitrogen (N_2), which was introduced into the cavity through the mirror mounts and evacuated by a set of gas curtains at the ends of the central bore. The gas curtains consisted of two sequential pump-out regions on either side of the bore, which ensured that sample gas did not flow from the central bore out to the arms of the cavity and to the mirrors. To provide adequate mirror protection from explosives vapor, the N_2 flow rate from the mirrors was set to approximately 100 sccm, exceeding the 10 sccm flow rate of sample gas that was injected into the bore. Furthermore, the pumping rate of the gas curtains was sufficiently high to accommodate the constant flow of N_2 from the mirrors, as well as the gas that was injected into the bore from the sample line. In addition, all surfaces that contacted explosives vapor were heated to 170 °C, and metal surfaces were passivated using a Silcosteel coating (Restek Corp.) to avoid condensation of explosives vapor in the cell.

A diode laser (Thor Labs, $\lambda = 635$ nm) was co-aligned with the idler output from the OPO to facilitate injection of the latter into the cavity. The OPO beam was mode-matched to the cavity mode using a 250-mm ZnSe lens. Light exiting the cavity was focused onto a liquid-nitrogen-cooled HgCdTe detector (Kolmar) using a 1-inch-focal-length ZnSe lens. Each ringdown trace was collected by a PC using a 100-MHz Gage card (CompuScope 12100). For each ringdown trace, the ringdown time constant, τ, was determined by a least-squares fitting routine. Ringdown times of $\tau = 20$ μs were typically measured. Five ringdown decay times were averaged per frequency step, yielding 1% fluctuation. This corresponded to an averaged sensitivity of 2×10^{-8} cm^{-1}, and, for a 25-Hz laser repetition rate, to a sensitivity of 9×10^{-9} cm^{-1} $Hz^{-1/2}$. Infrared spectra were obtained by measuring the ringdown time, τ, as a function of the angle of the ZGP crystal. The angle was then converted to a wavelength using an analytical form of the tuning curve shown in Fig. 2. Absolute wavelength calibration was obtained from a photoacoustic spectrum of water.

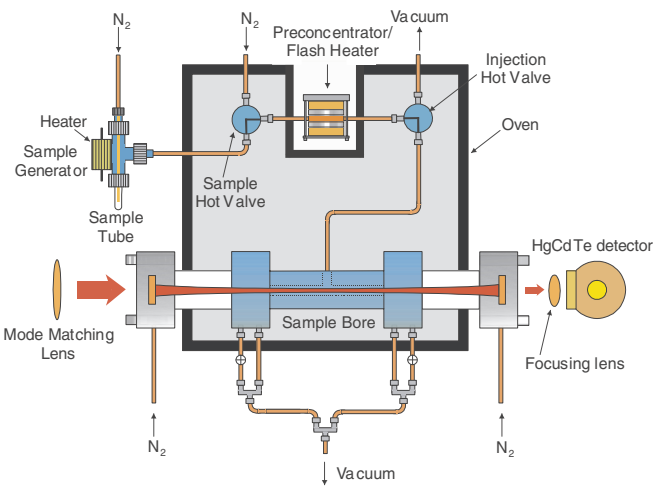

FIGURE 4 Schematic of the experimental set-up

An independently temperature-controlled sample generator was used as a source of explosives vapor. Samples were prepared by evaporating approximately 100 μl of explosives solution (Accustandard) in 4-mm I.D.×5 cm-length Pyrex sample tubes, leaving a thin film of explosives solid at the bottom of the tube. The sample tubes were attached to one end of a heated tee (170 °C), and an aluminum block, driven by a thermoelectric cooler (TEC), controlled the sample temperature over the range –5 to +200 °C. Explosives vapor was then entrained into a nitrogen (N_2) gas stream, with a flow rate of 10–30 sccm, that was controlled using MKS mass-flow controllers. The N_2 pick-up flow rate was kept low in order to ensure that the concentration of explosives vapor in the gas stream equaled the saturated vapor pressure of the sample generator. By varying the temperature of the sample tube, the resultant explosive vapor concentration in the output stream could be regulated. The resultant mixture was then delivered to a temperature-controlled, micro-finger preconcentrator.

The preconcentrator made use of a simple thermal cycle and the adsorption properties of explosives vapor to first collect a sample from the flowing stream onto a cooled surface, and then to subsequently rapidly release the accumulated sample back into the flow stream by means of flash heating. In this manner, explosive vapor could be collected from a relatively large volume of sampled gas, and released into a much smaller volume of gas to be injected into the CRDS cell, enhancing explosives vapor density by factors of 100 or more. A discussion of preconcentration is deferred to Sect. 4.3. The preconcentrator consisted of a thin-walled, Silcosteel-coated, stainless steel tube, passed through a Macor ceramic block and sandwiched between two TECs. The TECs provided cooling to the Macor block, which subsequently cooled the preconcentrator tube. In order to flash-heat the collector, 0.010″-thick gold wire was wrapped around the ends of the collector tubing and clamped down with brass lugs. Electrical leads were then attached to the lugs in order to provide 100 A of current though the tube. In this way, the sample tube could be heated to > 200 °C in less than 1 s. The low thermal conductivity of the Macor block allowed effective flash heating despite the constant cooling from the TECs, while also providing rapid cooling after the flash-heat cycle was completed.

The direction of gas flow was controlled via 3-way "hot valves", shown in Fig. 4. On the inlet side of the preconcentrator, one valve switched between the sample-bearing stream and the clean nitrogen flow. A similar three-way valve at the outlet of the preconcentrator toggled the gas flow either to be injected into the central bore of the CRDS cavity, or to be pumped away via a vacuum line. These valves were designed using polyetheretherketone (PEEK) plastic for the valve body and a specialized silicone seal, thus providing an inert sample environment, while also allowing for high temperature use (up to 200 °C). Switching of the valves

was accomplished using double air-actuation of a PEEK poppet.

The instrument was capable of running in two modes: "constant-flow" cycle, and "collection" cycle. In the "constant-flow" cycle, N_2 gas was continuously flowed through the sample generator and preconcentrator, and was then directed into the bore. The preconcentrator was heated to 170 °C so as not to collect any explosives. In this mode, a constant concentration of sample flowed through the ringdown cavity (controlled by the temperature of the sample generator), permitting infrared spectra to be acquired.

The "collection" cycle was employed for preconcentration measurements. Explosives concentrations in ambient air were orders of magnitude lower than those from the sample generator, and typically were below the detection limit of the instrument under the "constant-flow" mode. The "collection" cycle consisted of three steps. Firstly, the preconcentrator was cooled to –10 °C and the output stream from the sample generator was directed through the cold preconcentrator and then evacuated to a pump. Secondly, after a designated collection time, the "sample" hot valve was switched to purge the gas lines with clean N_2. Thirdly, following approximately 5 s of purge, the "injection" hot valve was switched to the bore. The preconcentrator was then flash heated to $\Delta T = 200$ °C, desorbing the collected explosives and delivering the sample to the cavity in a compact packet of gas.

4 Results and discussion

4.1 *Explosives detection limits*

Detection limits for the targeted explosives can be estimated by comparing the absorption coefficient for a given concentration of explosives to the sensitivity of the cavity-ringdown instrument (2×10^{-8} cm^{-1}). Absorption coefficients are calculated using,

$$\alpha(\lambda, T) = [\text{explosive}]_T \cdot \sigma_\lambda \,, \qquad (2)$$

where $\alpha(\lambda;T)$ is the absorption coefficient as a function of wavelength, λ, and temperature, T, $[\text{explosive}]_T$ corresponds to the concentration of explosives vapor at temperature T and σ_λ is the peak absorption cross-section at wavelength, λ. Table 1 lists these parameters along with the expected single-pass absorbances at room temperature for some common explosives. Given the instrument sensitivity of 2×10^{-8} cm^{-1}, TNT vapor at room temperature should be detectable. Without preconcentration, the absorption levels for RDX, PETN and Tetryl at room temperature are below the detection limits of the CRD system. However, with the 2- to 3-orders-of-magnitude enhancement in sample density expected from the preconcentrator, which will be discussed in Sect. 4.3, signal levels should be sufficient to detect these explosives at their room temperature vapor pressures, and TNT well below its saturated vapor pressure.

Explosive	Vapor pressure 298 K (moles/cm^3)[a]	σ (cm^2/mole)[b]	α (cm^{-1})
TNT	2.9×10^{-13}	5.1×10^{5}	1.5×10^{-7}
RDX	2.6×10^{-16}	7.8×10^{5}	2.0×10^{-10}
PETN	8.1×10^{-16}	1.4×10^{5}	1.1×10^{-10}
Tetryl	2.2×10^{-17}[c]	5×10^{5}[d]	1×10^{-11}

[a] [25]
[b] [26]
[c] [27]
[d] The absorption cross section for the symmetric stretching excitation of the –NO_2 groups in Tetryl is approximated to be similar to those of TNT, RDX and PETN

TABLE 1 Room-temperature vapor pressure, absorption cross section and absorbance of TNT, RDX, PETN and Tetryl. Reliable values for TATP are unavailable

4.2 *Mid-infrared spectra*

Vapor-phase cavity-ringdown spectra of several explosives were measured without sample preconcentration, in the wavelength range 7–8 μm. Each sample was prepared as described in the experimental section. The vapor was entrained in a N_2 flow and introduced continuously into the ringdown cavity. For each explosive, spectra were collected over a range of sample temperatures. It is important to note that varying the sample temperature is merely a means of controlling the concentration of explosives vapor in the N_2 carrier gas. All the infrared spectra presented here were obtained with the bore temperature held constant at 170 °C, that is, with the sample vapor at 170 °C.

Figure 5 shows the vapor phase spectrum of trinitrotoluene (TNT) obtained between 7 and 8 μm at sample temperatures ranging from 30 to 60 °C. The spectral features are well matched to published TNT vapor-phase absorption bands [26]. The spectrum is characterized by a strong absorption at 7.41 μm, corresponding to excitation of the symmetric stretch of the –NO_2 groups. A smaller feature grows in at 7.11 μm as the sample temperature is ramped, increasing the sample concentration in the bore. The peaks were fitted to model functions in order to extract approximate feature widths, and the results are listed in Table 2. The full-width at half-maximum (FWHM) of each vibrational band at 170 °C

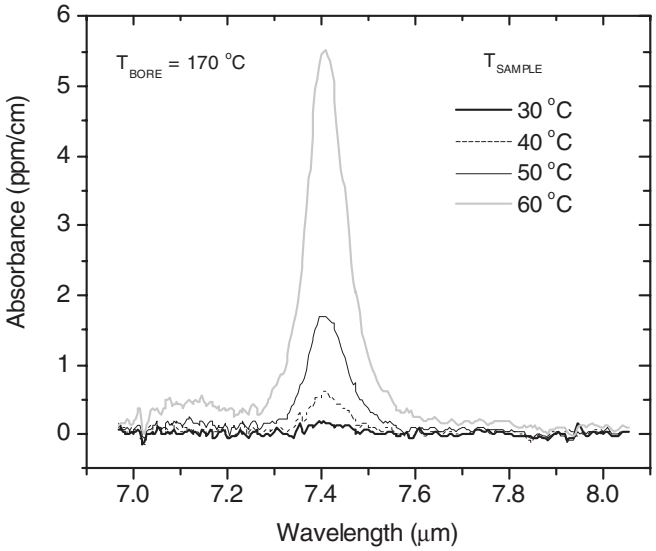

FIGURE 5 Vapor phase spectrum of TNT between 7 and 8 μm

	Band (cm^{-1})	FWHM (cm^{-1})
TNT	1349.3 ± 0.1	17.5 ± 0.8
	1406.7 ± 0.5	–
RDX	1274.2 ± 0.1	24.9 ± 1.2
	1306.0 ± 0.1	–
	1351.5 ± 0.6	–
	1386.9 ± 0.4	–
PETN	1284.3 ± 0.1	21.0 ± 1.0
	1376.4 ± 0.5	–
TATP	1275.3 ± 0.4	20.9 ± 1.0
	1375.8 ± 0.1	–
Tetryl	1292.3 ± 0.4	24.6 ± 1.4
	1347.0 ± 0.1	–

TABLE 2 Model widths of observed mid-infrared vibrational bands for TNT, RDX, PETN, TATP and Tetryl

is $17.5 \pm 0.8\,cm^{-1}$. At a sample tube temperature of $T = 25\,°C$, a CRD absorption strength of $0.12 \pm 0.02\,ppm\,cm^{-1}$ ($1.2 \times 10^{-7}\,cm^{-1}$) is observed for the 7.41 μm band. The absolute value of this signal agrees closely with the expected room temperature TNT absorption, $1.5 \times 10^{-7}\,cm^{-1}$, as listed in Table 1.

In a similar way, mid-IR spectra of RDX, PETN, triacetone triperoxide (TATP), and nitramine (Tetryl) were measured and are shown in Fig. 6. Each spectrum is unique and shows prominent features in the range 7–8 μm. FTIR spectra of RDX and PETN were also collected and agree well with those presented here [27]. The high volatility of TATP allows it to be detected at temperatures as low as –5 °C. In contrast, the low vapor pressures of RDX, PETN and Tetryl required substantial heating of the sample to achieve detectable levels in the CRD cell. Results of the spectral fits are shown in Table 2. As expected, the widths of the features are species dependent (different transition types, rotational constants etc.), which, when coupled with the peak positions, provide a set of unique parameters to be used in spectral identification algorithms.

4.3 *Sample preconcentration*

As discussed above, concentration enhancements by a factor of 10^2–10^3 are necessary in order to detect ambient levels of low-vapor-pressure explosives like RDX and PETN. Preconcentration is achieved using a temperature cycle where explosives vapor from a given sampling volume is condensed onto a cold finger and subsequently released as a condensed packet of gas into the cavity by flash heating the cold finger. The degree of preconcentration is related the ratio of the volume of gas sampled to the volume of the sample cell into which the condensed gas packet is injected, and therefore depends upon the sampling flow rates and sampling time, as well the specific explosive vapor utilized. In the current experimental set-up, the sample generator was attached to the preconcentrator in order to test the collection and flash heating efficiencies, as described later. Clearly, preconcentration factors would be small using the

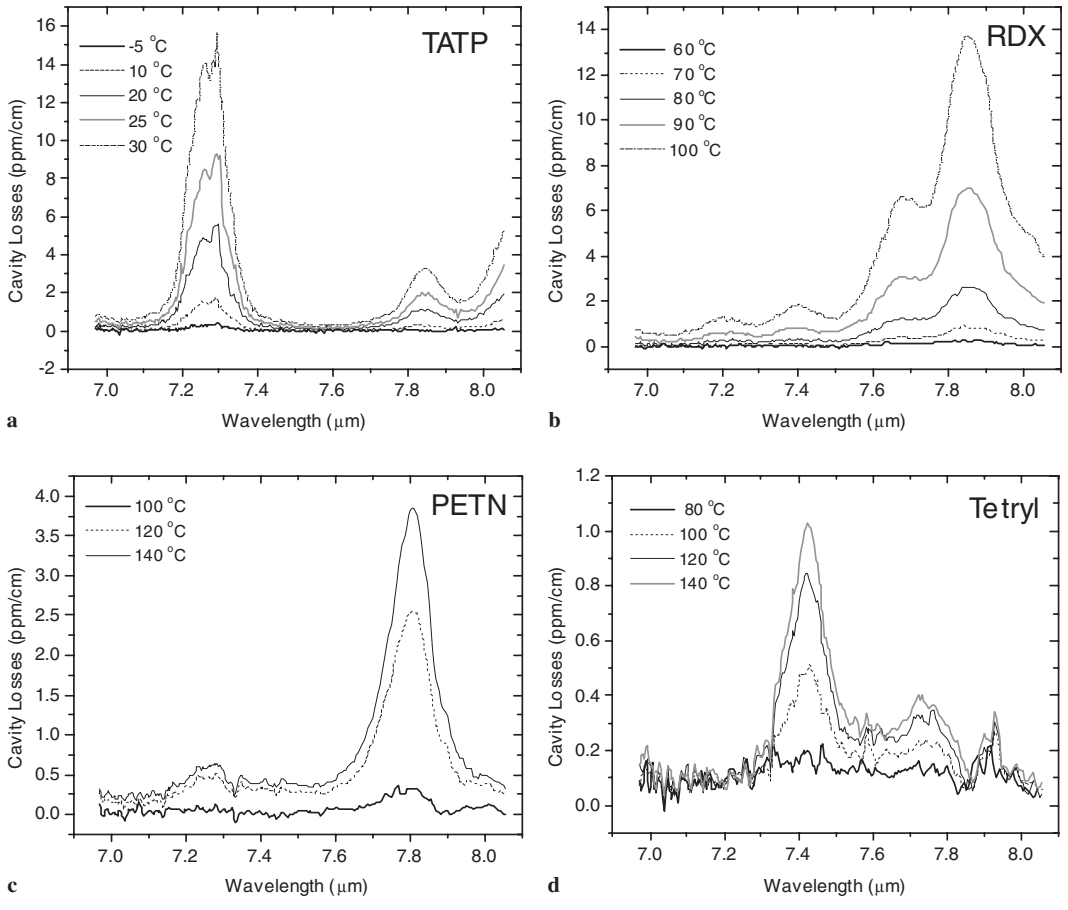

FIGURE 6 Vapor phase spectra of: **a** TATP; **b** RDX; **c** PETN; and **d** Tetryl

low gas flow exiting the sample generator. A 10-s collection time of gas flowing at 30 sccm from the sample generator equals a sample volume of 5 cm^3 which matches exactly the 5 cm^3 sample cell volume, resulting in no explosives vapor preconcentration. The effectiveness of the preconcentrator will be realized with ambient air sampling, which is discussed in Sect. 4.4. Sample flow rates of the order of 1000–5000 sccm will be used, which translates into a sampling volume of 160–830 cm^3 over a 10-s collection time. This corresponds to preconcentration factors of 30–160. Preconcentration can be further enhanced with longer collection times.

The performance and sensitivity of this instrument may be analyzed and described in several ways. Since this instrument is designed to directly sample an ambient gas stream, one logical way to define the overall sensitivity to a given explosive is the minimum concentration that is detectable in a given sampling time – i.e. X ppb of explosive Y in t seconds. Another common way to describe instrument sensitivity is via the minimum detectable mass for a given explosive – i.e. Z pg of explosive Y [28]. This latter form is common for particle sampling systems (particularly IMS-based systems), but is less applicable to gas sampling systems because of the neglected factor of collection time. In general, the minimum detectable amount can be related to the minimum detectable absorbance by: [Minimum Detectable Absorbance] = [Amount Sampled] × [Fraction Transferred to Bore] × [Absorption Strength].

Since we wish to express this as a minimum concentration that is detectable in a given sampling time – i.e. X ppb of explosive Y in t seconds:

$$\alpha_{\mathrm{MIN}} = \left[X_{Y,\mathrm{min}} \frac{P^0}{kT^0} F_{\mathrm{SAMP}} t \right] \times [\eta_{\mathrm{C}} \eta_{\mathrm{FH}} \eta_{\mathrm{INJ}}] \times \left[\frac{\sigma_{\mathrm{Y}}}{V_{\mathrm{BORE}}} \right] \quad (3)$$

where α_{MIN} is the minimum detectable absorbance, $X_{Y,\mathrm{min}}$ is the minimum detectable ambient concentration of explosive Y, P^0 and T^0 are the standard pressure and temperature, F_{SAMP} is the sampling standard flow rate, t is the sampling time, η_{C} is the collector efficiency, η_{FH} is the flash heating efficiency, η_{INJ} is the injection efficiency, σ_{Y} is the absorption cross-section of explosive Y and V_{BORE} is the volume of the sample bore.

In order to predict the minimum detection limit of explosives, the system dependent parameters η_{C}, η_{FH}, and η_{INJ} first need to be evaluated. The first two terms (η_{C}, η_{FH}) are considered below, while the third (η_{INJ}) has been conservatively estimated to be 0.9.

4.3.1 Collector efficiency (η_{C}). The collector efficiency is defined as the percentage of explosives vapor that enters the chilled collector and adsorbs onto the inner surface of the tube. During a collection cycle, any explosives vapor that leaks through the tube is a loss, and degrades sensitivity. To evaluate the collector efficiency, the instrument was operated in constant-flow mode, and the sample generator and collector temperature were cycled. The graph in Fig. 7 displays the absorption signal, monitored at the peak of the TNT absorption feature (7.41 μm) as a function of time. Initially, the TNT sample was cooled to 10 °C, providing an undetectable level of vapor, and the collector was heated to 170 °C in order to pass TNT vapor through to the cell. With no detectable TNT vapor, this defined the baseline losses at 1.4 ppm/cm. The sample tube was then heated to 60 °C (while the collector was maintained at 170 °C), generating a substantial concentration of TNT vapor, and a signal absorbance of 6.5 ppm/cm was recorded. In order to test the collection efficiency of the preconcentrator, the collector tube was then cooled to –10 °C. The absorption promptly decreased until a baseline ringdown time was recovered, indicating effectively 99% (considering the 1% uncertainty) collection efficiency of TNT vapor, or in other words, $\eta_{\mathrm{C}} = 0.99$. The collection efficiencies of RDX and some TNT decomposition products, o-nitrotoluene (MNT) and 2,4-dinitrotoluene (DNT), were also 99%, and it is assumed that collection of other explosives will be similar.

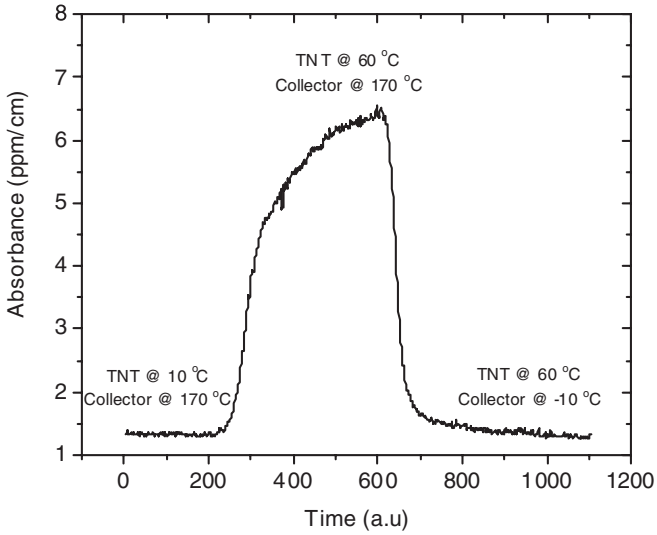

FIGURE 7 Preconcentrator collection efficiency. OPO wavelength was fixed at 7.41 μm while the temperatures of the TNT sample and the collector tube were varied

4.3.2 Flash-heat efficiency (η_{FH}). The next step in the preconcentration cycle is to deliver the collected explosives molecules to the central bore in a compact packet of gas. This is realized by flash heating the collector tube, thereby desorbing the explosives, and then flowing N_2 purge gas to inject the vapor into the CRD cavity. The effectiveness of the flash heating cycle was tested in order to ensure complete desorption of explosives molecules from the collector tube, as well as to perfect transfer into the CRD cell. In this test, the instrument was cycled through a series of purge, collect, and flash-heat modes, with the TNT sample chilled to 10 °C and the collector tube to –10 °C. The results are shown in Fig. 8 where, again, the absorption signal was monitored at the peak of the TNT absorption feature (7.41 μm) as a function of time. Initially, the hot valves were switched for a collection cycle. After 30 s of collection time, where N_2 flowed from the sample generator, through the preconcentrator and out to a vacuum pump, the sample hot valve was switched to a purge cycle, and N_2 purge gas flowed through the preconcentrator. After a few seconds, the injection hot valve was switched to the bore, and the preconcentrator was flash-heated. A large pulse of TNT vapor was instantly injected into the cavity. With

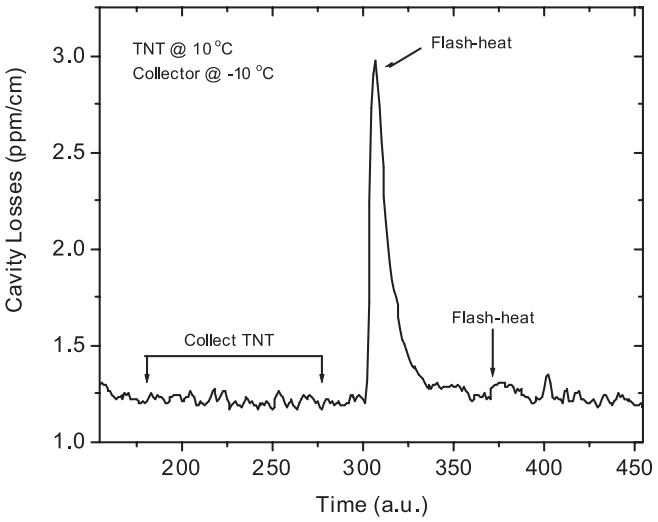

FIGURE 8 Flash-heat efficiency. Collector was chilled to –10 °C and laser was fixed at 7.41 μm

a constant flow of N_2 into the bore, the TNT was quickly flushed through the bore. Approximately 10 s after the primary flash heat, a second flash heating of the collection tube was performed showing that very little, if any, TNT remained in the collector after the primary flash-heat cycle. The flash-heat efficiency in this case was greater than 95% ($\eta_{FH} > 95\%$). Again, experiments were conducted with RDX, MNT and DNT and provided similar flash-heat efficiencies. It is assumed that the flash efficiency of other explosives will be comparable.

With the efficiency terms known, the minimum detection limit of explosives can be calculated using (3). For example, under typical experimental conditions using a sample generator listed in the first column of Table 3, and a 10-s collection time, the minimum detectable concentration of TNT, $X_{TNT,\,min}$, is 1.2 ppb, and corresponds to its saturated vapor pressure at 12 °C [27]. This concentration is much higher than those anticipated in real-world conditions. However, the low flow rates required by the sample generator limit the effectiveness of the preconcentrator. The sampling volume in this case was 5 cm^3 (30 sccm over 10 s), which equaled the sample volume in the cavity, yielding a preconcentration factor of 1. In order to detect ambient levels of TNT, as well as other explosives, greater sampling volumes are necessary in order to increase the preconcentration factor.

Parameter	Sample generator	Membrane separator
α_{MIN}	2×10^{-8} cm^{-1}	2×10^{-8} cm^{-1}
F_{SAMP}	30 sccm	1 slpm
t	10 s	10 s
η_C	0.99	0.99
η_{FH}	0.95	0.95
η_{INJ}	0.9 (estimated)	0.9 (estimated)
η_{MS}	–	0.5
σ_{TNT}	7.71×10^{-19} cm^2/molecule	7.71×10^{-19} cm^2/molecule
V_{BORE}	5.0 cm^3	5.0 cm^3
$X_{TNT,\,min}$	1.2 ppb	75 ppt

TABLE 3 Minimum detectable TNT concentration, $X_{TNT,\,min}$, under typical experimental conditions, using a sample generator and membrane separator

4.4 *Ambient air sampling*

The ultimate purpose of this instrument is to detect trace levels of explosives vapor in ambient air. To this end, the sample generator was replaced with a membrane separator. This unit permits a relatively large volume of air to be sampled, and largely separates the explosive vapors from the ambient air components, especially water vapor. This separation is achieved by using a two-stage, semi-permeable membrane made of dimethyl-silicone (0.001″ thick). The gas permeability for this membrane material is a strong function of the boiling point of the vapor component, and a weaker function of the polarity of the molecules. For the primary air components such as N_2 and O_2 the permeability is relatively low ($P(N_2) = 2.5 \times 10^{-9}$ $cm^3/cm\,s\,cm^2$ Torr, $P(O_2) = 5.0 \times 10^{-9}$ $cm^3/cm\,s\,cm^2$ Torr). The permeability for water vapor is approximately two orders of magnitude higher than that of the primary air components, $P(H_2O) = 3.0 \times 10^{-7}$ $cm^3/cm\,s\,cm^2$ Torr, and the permeability for explosive compounds is estimated to be one to two orders of magnitude higher than that of water vapor [29]. The overall effect of the strong difference in permeability is a relatively rapid ($\sim$ 1 s) diffusion of explosive vapors across the membrane, a high rejection of water vapor, and almost no transfer of the primary air components (N_2 and O_2).

Preliminary tests of the membrane separator indicate successful transfer of explosive vapor across the membrane separator. Initial tests were carried out with samples of 2,4-dinitrotoluene (DNT) due to the enhanced vapor pressure compared with TNT or other explosives. Firstly, the spectrum of DNT was measured without the membrane separator, in the same fashion as the spectra of other explosives that are shown in Figs. 5 and 6. The spectrum of DNT is shown in Fig. 9 with the DNT sample heated to 40 °C. The sample generator was then placed at the inlet of the mem-

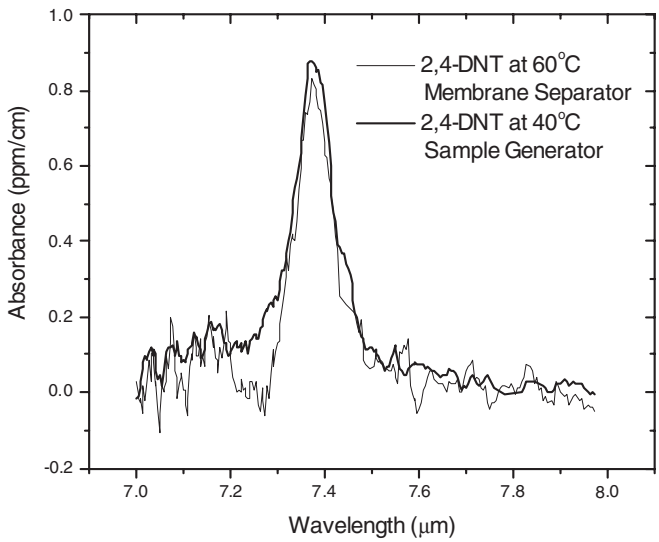

FIGURE 9 Vapor-phase spectrum of DNT measured with and without the membrane separator

brane separator, and a 10-sccm flow of DNT vapor was bled into an air stream that flowed past the membrane separator at 1000 sccm. Due to the 100-fold dilution of DNT in the gas stream, the sample was heated to 60 °C for enhanced concentration. Figure 9 compares the spectrum of DNT using the two configurations. There is more water vapor in the sample stream when using the membrane separator, exhibited by the higher noise in the spectrum, particularly between 7.0 and 7.3 μm. The suppression of water is nonetheless impressive, making the detection of explosives possible. By comparison, without any water suppression from the membrane separator, the concentration of water vapor in ambient air would quench any ringdown signal.

By design, the maximum efficiency of the membrane separator is $\eta_{MS} = 0.5$, and the actual efficiency ought to be very close to the optimum value. Once experimentally determined, the coefficient, η_{MS}, can be inserted into (3) and the minimum detectable amount of explosives vapor in the ambient air can be calculated. Much higher sampling flow rates are possible using a membrane separator, which greatly increases the sensitivity of the instrument due to enhanced preconcentration. With the expected experimental conditions listed in the second column of Table 3, and using a membrane separator efficiency of $\eta_{MS} = 0.5$, the minimum detectable limit of TNT vapor drops from 1.2 ppb using a sample generator, to 75 ppt using a membrane separator that samples ambient air. Similar concentrations of RDX, PETN and other explosives are expected to be detectable due to similar absorption cross-sections.

4.5 *Spectral identification*

Along with the demonstrated instrument sensitivity for explosives vapor detection, recognition algorithms must be developed not only to identify the target explosives, but also distinguish them from a large number of interferents. Spectral features of non-explosive compounds may partially overlap with target spectra. The most obvious means of distinguishing explosives from non-explosive compounds, as well as uniquely identifying the target explosive, is to create a spectral library of explosives and interferents that contains peak positions and lineshapes. Table 1 lists some spectral data for select explosives between 7 and 8 μm. While the spectral signatures of these explosives are distinct, many of the spectra contain only a single feature, which will not allow them to be distinguished from interferents that absorb in the same region. To this end, the spectral library of the target explosives is currently being expanded to span 6 to 8 μm. With the additional spectral features recorded between 6 and 7 μm, unique signatures of the target explosives will be obtained. Similarly, a spectral library of potential interferents is also being collected between 6 and 8 μm. To date, spectra of over 25 compounds have been recorded and analyzed, with most spectra exhibiting broad features. While a comprehensive library of interferents is desired, it is impossible to guess the full set of compounds needed. Furthermore, with an excessively large spectral library of interferents, it will become increasingly difficult to positively identify an explosive compound from a collection of interferents. Therefore, only the most common compounds will be included in the library at first, with additional species to be added as necessary.

Identification of explosives vapor must be made in approximately 10 to 20 s, as requested by the TSA. In this time, the sample must be collected and flash-heated into the ringdown cavity, spectra must be measured and then analyzed for identification. With such a short sampling time, it is not possible to record a full spectrum between 6 and 8 μm. Rather, absorption strengths will be measured at discreet wavelengths. Then, recognition algorithms will rely on the data from the spectral library, including the lineshapes of the spectral features, in order to identify explosives.

Among the interferents, water is by far the most prevalent, with narrow, strongly absorbing lines. The spectral width of water lines is $0.07\,cm^{-1}$/atm, which is much narrower than the $2\,cm^{-1}$ laser linewidth. The laser linewidth is an envelope of approximately 30 discreet laser modes, spaced by $0.07\,cm^{-1}$. The population of the laser cavity modes within the $2\,cm^{-1}$ linewidth fluctuates significantly, so that the interaction of a given mode with a water line is random. This random absorption gives a poorly reproducible water spectrum, and appears as noise in the data. One possible solution to overcoming the issue of water interference is to develop an algorithm based on robust estimation, which monitors the standard deviation of collected ringdown times. The random interaction of a laser mode with a water line will appear as an outlier in the averaged set of decay times, and can therefore be discarded. In principle, the "true" absorption (i.e. the absorption without any water interference) can be extracted. Ongoing analysis will determine the appropriateness of such an approach.

Very recent data indicate that by cooling the preconcentrator tube during a collection cycle to only 5 °C rather than –10 °C, minimal water is collected, and therefore very little is injected into the ringdown cavity with the explosives vapor. This suggests that there is essentially complete separation of water vapor from the explosives sample, which will greatly reduce the burden on the recognition algorithms.

5 Conclusions

A broadly tunable mid-IR laser source has been developed and has been applied to the trace detection of explosives vapor using mid-IR cavity-ringdown spectroscopy. The laser source is a ZGP OPO, operational in the idler wave between 6 and 10 μm, and is pumped at 2.8 μm by a 25-Hz Er,Cr:YSGG laser. The idler output beam profile is nearly Gaussian, with a beam divergence close to the diffraction limit. Between 6 and 8 μm, the output energy reaches 300 μJ/pulse with an average linewidth of approximately $2\,cm^{-1}$.

Mid-IR spectra between 7 and 8 μm have been recorded for a variety of explosives. FTIR spectra have also been recorded to verify those recorded by CRDS, and the agreement is good. In addition, the signal levels are consistent with theoretical expectations based on vapor pressures and absorption cross-sections [25, 26].

The sensitivity of our CRDS set-up ($2 \times 10^{-8}\,cm^{-1}$), along with the strong absorption cross sections of the funda-

mental vibrational bands in the mid-IR, provides an excellent means of detecting trace levels of explosives vapor. For explosives with very low vapor pressures (e.g. RDX, PETN and Tetryl), the ambient concentrations fall below the sensitivity of the instrument; therefore, a preconcentrator has been implemented to enhance the explosives vapor concentration by factors of 100 or more. Collection efficiencies onto the preconcentrator cold finger of 99% have been demonstrated, as well as excellent flash heating and desorption efficiencies (95%). Initial tests carried out at reduced pressures (100 Torr) reveal baseline sensitivities of approximately 1.2 ppb of TNT, and comparable levels for other explosives.

The addition of a membrane separator at the inlet of the gas sampling line permits ambient samples to be tested. With optimum separation of explosives vapor from interferents in air (mainly water vapor), early tests suggest that concentrations as low as 75 ppt are detectable for TNT (and similar levels for RDX, PETN and other explosives with similar absorption cross sections), or equivalently, 600 pg [30].

Future work includes the development of a CW mid-IR laser source. CW lasers have significantly lower noise levels than pulsed lasers, where a sensitivity level of $1.0 \times 10^{-12}\,\mathrm{cm}^{-1}\,\mathrm{Hz}^{-1/2}$ has been achieved in a CW CRDS experiment [23] utilizing a low-excess-noise analog detection system operating at a high signal acquisition rate. Relative measurement errors of $\delta\tau/\tau = 0.1\%$ can readily be achieved, thereby increasing the sensitivity in this experiment by an order of magnitude.

Applications of this instrument are by no means limited to the detection of explosives. A primary objective at Picarro is to extend this technology to trace detection of other illicit substances such as drugs (crack, cocaine, LSD, amphetamines), and chemical/biological warfare agents (tabun, sarin, mustard gas, VX). Existing FTIR spectra of these substances exhibit similar spectroscopic characteristics as explosives, such as strong, fundamental vibrational bands in the mid-IR as well as similar vibrational band profiles. With such a broad tuning range of the OPO laser, extending the application of our instrument to the detection of these substances can be realized by optimizing the optics for the wavelength range necessary, and by modifying the recognition algorithms to identify the proper spectral signatures.

ACKNOWLEDGEMENTS The work described in this paper has been carried out as a collaborative effort between M.I.T. and Picarro, Inc., supported through Cooperative Research Agreement No. 00-G-021 from the Federal Aviation Administration Office of Research and Technology Application, and through Cooperative Research Agreement No. 70NANB9H3017 from the National Institute of Standards and Technology (Advanced Technology Program).

REFERENCES

1 J.I. Steinfeld, J. Wormhoudt: Ann. Revs. Phys. Chem. **49**, 203 (1998)
2 An example of a commercial X-ray CT device, the InVision CTX 5500 by InVision Technologies, Newark CA, may be found at http: //invision-tech.com/products
3 A. Fainberg: Science **255**, 1531 (1992)
4 M. Fischetti: Technol. Rev. **100**, 39 (1997)
5 P. Kolla: Angew. Chem. Int. Ed. Engl. **36**, 800 (1997)
6 Z.P. Sawa: Nucl. Instrum. Methods Phys. Res. B **79**, 593 (1993)
7 R.A. Strobel, R. Noll, C.R. Midkiff Jr.: Proc. 4th Int. Symp. Anal. Detect. Explos. in Jerusalem, Israel, Sept. 7–10, 1992 (Kluwer Academic, 1993) p. 455
8 S. Lovett: Proc. 1st Int. Symp. Explosive Detection Technology in Atlantic City, NJ, USA, Nov. 13–15, 1991, p. 774
9 For examples of IMS commercial instruments in use at airports, see the following websites: http: //www.barringer.com/html/ionscan_400b.html; http: //www.airport-technology.com/contractors/security/barringer/; http: //www.iontrack.com/itemiser.html
10 M.P. Jacobson, S.L. Coy, R.W. Field: J. Chem. Phys. **107**, 8349 (1997)
11 A. O'Keefe, D.A.G. Deacon: Rev. Sci. Instrum. **59**, 2544 (1988)
12 A. O'Keefe, J.J. Scherer, A.L. Cooksy, R. Sheeks, J.R. Heath, R.J. Saykally: Chem. Phys. Lett. **172**, 214 (1990)
13 J.J. Scherer, D. Voelkel, D.J. Rakestraw, J.B. Paul, C.P. Collier, A. O'Keefe, R.J. Saykally: Chem. Phys. Lett. **245**, 273 (1995)
14 J.B. Paul, R.A. Provencal, C. Chapo, K. Roth, R. Casaes, R.J. Saykally: J. Phys. Chem. A **103**, 2972 (1999)
15 D.D. Romanini, K.K. Lehman: J. Chem. Phys. **99**, 6287 (1993)
16 P. Zalicki, R.N. Zare: J. Chem. Phys. **102**, 2708 (1995)
17 J.T. Hodges, J.P. Looney, R.D. van Zee: J. Chem. Phys. **105**, 10278 (1996)
18 J. Martin, B.A. Paldus, P. Zalicki, E.H. Wahl, T.G. Owano, J.S. Harris Jr., C.H. Kruger, R.N. Zare: Chem. Phys. Lett. **258**, 36 (1996)
19 R.D. van Zee, J.T. Hodges, J.P. Looney: Appl. Opt. **38**, 3951 (1999)
20 D. Romanini, A. Kachanov, N. Sadeghi, F. Stoeckel: Chem. Phys. Lett. **270**, 538 (1997)
21 B.A. Paldus, C.C. Harb, T.G. Spence, B. Wilke, J. Xie, J.S. Harris, R.N. Zare: J. Appl. Phys. **83**, 3991 (1998)
22 T.G. Spence, C.C. Harb, B.A. Paldus, R.N. Zare, B. Wilke, R.L. Byer: Rev. Sci. Instrum. **71**, 347 (2000)
23 K.W. Busch, M.A. Busch (Eds.): *Cavity-Ringdown Spectroscopy: An Ultratrace-Absorption Measurement Technique, ACS Symposium Series* (Oxford University Press, Oxford 1999)
24 K.L. Vodopyanov, F. Ganikhanov, J.P. Maffetone, I. Zwieback, W. Ruderman: Opt. Lett. **25**, 841 (2000)
25 B.C. Dionne, D.P. Rounbehler, E.K. Achter, J.R. Hobbs, D.H. Fine: J. Energetic Mater. **4**, 447 (1986)
26 J. Janni, B.D. Gilbert, R.W. Field, J.I. Steinfeld: Spectrochim. Acta A **53**, 1375 (1997)
27 C. Harper, F. Llados: *Toxicological Profile for Tetryl* (Research Triangle Institute) (U.S. Department of Health and Human Services 1995)
28 In this case, a substitution of the first term in (3) is made where Z_Y is the mass of explosive Y, M_Y is its molecular weight and N_A is Avogadro's number: $\alpha_{MIN} = \left[\frac{Z_Y}{M_Y} N_A\right] \times [\eta_c \eta_{FH} \eta_{INJ}] \times \left[\frac{\sigma_Y}{V_{BORE}}\right]$
29 Permeabilities for this membrane are published by the manufacturer and can be found at http: //www.sspinc.com/membranes_spec.cfm
30 The equation in [28] was used to estimate the minimum detectable mass, with $\eta_{MS} = 0.5$